The internal magnetic field in a ferromagnetic compound Y<inf>2</inf>Co<inf>12</inf>P<inf>7</inf>

The internal magnetic field in a ferromagnetic compound $Y_2Co_{12}P_7$

Journal of Physics: Conference Series **2462** (2023) 012008 doi:10.1088/1742-6596/2462/1/012008

The internal magnetic field in a ferromagnetic compound $Y_2Co_{12}P_7$

Kazuki Ohishi[1,*], Hiroto Ohta[2], Yusuke Kato[3], Hiroko Aruga Katori[3], Ola K. Forslund[4], Elisabetta Nocerino[5], Nami Matsubara[5], Papadopoulos Konstantinos[4], Fredrik O. L. Johansson[6,7], Yasmine Sassa[4], Martin Månsson[5], Bassam Hitti,[8] Donald Arseneau[8], Gerald D. Morris[8], Jess H. Brewer[9], Jun Sugiyama[1,*]

[1] Neutron Science and Technology Center, Comprehensive Research Organization for Science and Society (CROSS), Tokai, Ibaraki 319-1106, Japan
[2] Faculty of Science and Engineering, Doshisha University, 1-3 Tatara Miyakodani, Kyotanabe-shi, Kyoto 610-0321, Japan
[3] Department of Applied Physics, Tokyo University of Agriculture and Technology, 2-24-16 Naka-cho, Koganei-shi, Tokyo 184-8588, Japan
[4] Department of Physics, Chalmers University of Technology, SE-412 96 Göteborg, Sweden
[5] Department of Applied Physics, KTH Royal Institute of Technology, Roslagstullsbacken 21, SE-106 91 Stockholm, Sweden
[6] Department of Physics and Astronomy, Ångströmlaboratoriet, Uppsala University, SE-75120 Uppsala, Sweden
[7] Department of Chemistry, KTH Royal Institute of Technology, SE-100 44 Stockholm, Sweden
[8] TRIUMF, 4004 Wesbrook Mall, Vancouver, BC, V6T 2A3 Canada
[9] Department of Physics & Astronomy, University of British Columbia,Vancouver, BC, V6T 1Z1 Canada

E-mail: k_ohishi@cross.or.jp, juns@triumf.ca, or j_sugiyama@cross.or.jp

Abstract. The internal magnetic field in a ferromagnetic compound, $Y_2Co_{12}P_7$ with T_C = 150 K, was studied with μ^+SR using a powder sample down to 2 K. The wTF-μ^+SR measurements revealed the presence of a sharp magnetic transition at T_C = 151 K, and the ZF-μ^+SR measurements clarified the formation of static magnetic order below T_C. The presence of two muon spin precession signals in the ZF-μ^+SR spectrum below T_C indicates the existence of the two different muon sites in the lattice. By considering the muon sites and local spin densities at the muon sites predicted with DFT calculations, the ordered magnetic moments of Co were successfully determined.

1. Introduction

An internal magnetic field at the μ^+ site ($\boldsymbol{H}_{\mathbf{int}}$) in antiferromagnets is usually equivalent to a dipole field ($\boldsymbol{H}_{\mathbf{dip}}$), while $\boldsymbol{H}_{\mathbf{int}}$ in ferromagnets are given by the sum of a dipole field ($\boldsymbol{H}_{\mathbf{dip}}$), a Lorentz field ($\boldsymbol{H}_{\mathbf{L}}$), and a hyperfine field ($\boldsymbol{H}_{\mathbf{hf}}$) [1, 2]. In other words, $\boldsymbol{H}_{\mathbf{L}} = \boldsymbol{H}_{\mathbf{hf}} = \mathbf{0}$ for antiferromagnets. Recently, not only the muon sites but also $\boldsymbol{H}_{\mathbf{hf}}$ are predicted for various ferromagnets with first principles calculations, leading to more precise analyses of the μ^+SR data for ferromagnets. This could be an advantage of μ^+SR over neutron scattering, because ferromagnetic Bragg peaks are overlapped with nuclear peaks. Therefore, it is a good challenge

to study $\boldsymbol{H}_{\mathbf{int}}$ in ferromagnets with μ^+SR [3, 4, 5, 6, 7], particularly for the compounds possessing two different magnetic moments.

The target compound $Y_2Co_{12}P_7$ belongs to a hexagonal symmetry with space group $P\bar{6}$ (see Fig. 1) and enters a ferromagnetic state at $T_C = 150$ K. A series of $R_2Co_{12}P_7$ compounds, where R denotes a rare earth element, were originally synthesized in 1978 by a solid state reaction in an evacuated silica tube for 7 days at 1070 K [8]. The magnetic properties were reported by magnetization and neutron scattering measurements [9, 10]. As a result, the ordered magnetic moment of Co ($\boldsymbol{m}_{\mathrm{Co}}$) was found to align along the c-axis regardless of R in the FM state, while the magnitude and direction of the ordered rare earth element ($\boldsymbol{m}_R$) strongly depend on the number of f electrons: for example, $\boldsymbol{m}_{\mathrm{Nd}}$ is antiparallel to $\boldsymbol{m}_{\mathrm{Co}}$, but $\boldsymbol{m}_{\mathrm{Ho}}$ is parallel to $\boldsymbol{m}_{\mathrm{Co}}$, and $\boldsymbol{m}_{\mathrm{Pr}}$ is canted from the c-axis, for reasons currently unknown. Prior to a systematic μ^+SR work on $R_2Co_{12}P_7$, we have attempted to study $\boldsymbol{H}_{\mathbf{int}}$ in $Y_2Co_{12}P_7$ at first, because of the absence of d nor f electron of Y^{3+}.

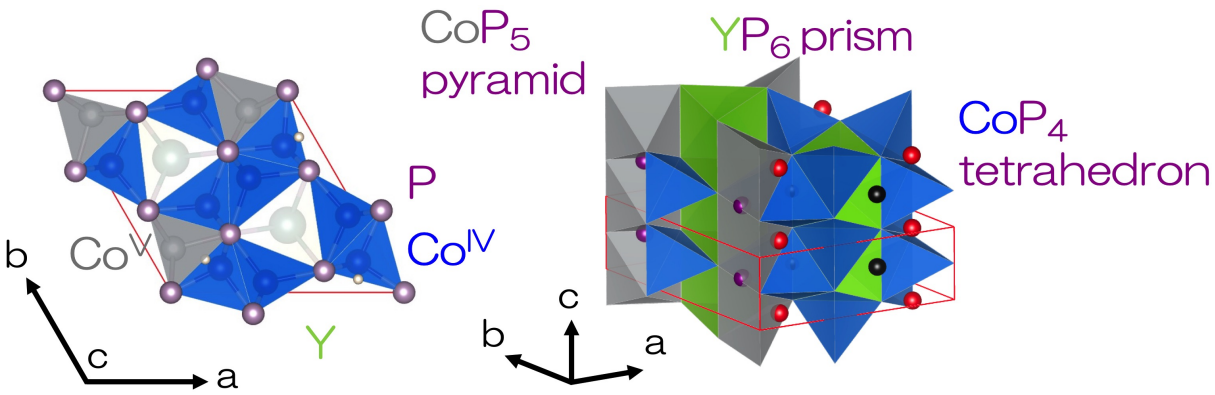

Figure 1. The crystal structure of $Y_2Co_{12}P_7$. Among the four different Co sites in the lattice, i.e., Co1, Co2, Co3, and Co4 sites, the former three sites (Co1, Co2, and Co3) are classified as a tetrahedral site, while the latter site (Co4) is a pyramidal site. In the right figure, small spheres represent the predicted three muon sites with first principles calculations: that is, $\mu_1 = (0.22950, 0.1639, 0)$ (red), $\mu_2 = (0.41667, 0.3166, 0.5)$ (black), and $\mu_3 = (0.08333, 0.2166, 0.5)$ (magenta).

2. Experimental

A powder sample of $Y_2Co_{12}P_7$ was prepared by a solid state reaction technique in Tokyo University of Agriculture and Technology [11], using a similar way described in Ref. [8]. That is, powder of Y (purity 3N), Co (purity 3N), and P (purity 6N) were mixed and then heated at 1000 °C for 12 h in evacuated silica tubes. Obtained reactant was well grounded and heated at 1200 °C for 12 h in evacuated silica tubes. The crystal structure of the sample was determined by a powder X-ray diffraction analysis. The temperature dependence of magnetization was measured with a superconducting quantum interference device (SQUID) magnetometer (MPMS, Quantum Design) [11, 12].

The μ^+SR spectra were measured on the M20 surface muon beam line using the LAMPF spectrometer at TRIUMF in Canada. An approximately 200 mg powder sample was placed in a 1×1 cm^2 square envelope made from 0.05 mm thick aluminized Mylar tape in order to minimize the signal from the envelope. The envelope was attached to a low-background sample holder in a liquid-He flow-type cryostat for measurements in the temperature range between 2 and 250 K. The muon site(s) and the local spin density at the muon site(s) ρ_{spin} were predicted with DFT

calculations using a full-potential linearized augmented plane-wave method within generalized gradient approximations as implemented in WIEN2k program package [13]. The experimental techniques are described in more detail elsewhere [14, 2]. The obtained μ^+SR spectra were analyzed using musrfit [15].

3. Results and Discussion

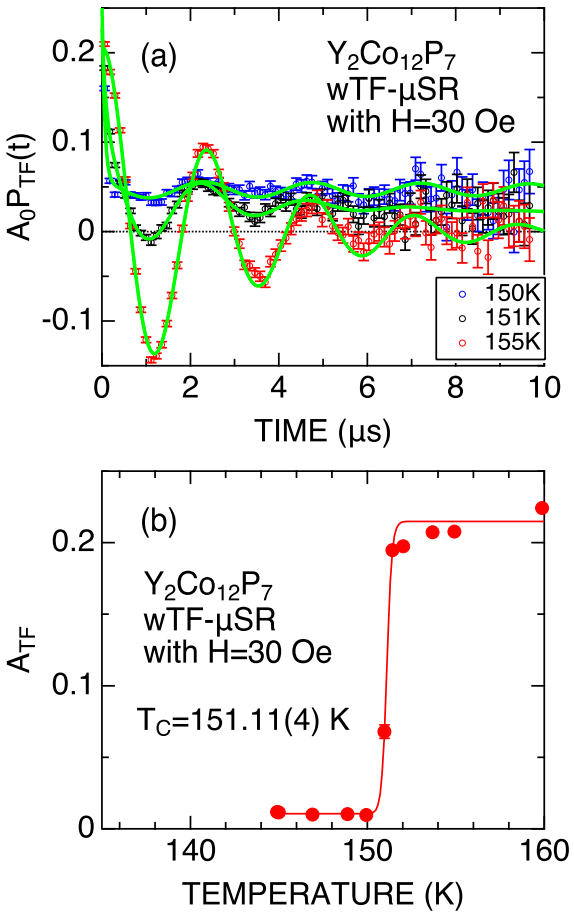

Figure 2. (a) The temperature variation of the wTF-μ^+SR spectrum in $H_{\rm TF} = 30$ Oe recorded at 155, 151, and 150 K and (b) the temperature dependence of the wTF asymmetry ($A_{\rm TF}$) for $Y_2Co_{12}P_7$. In (a) solid lines represent the best fit using Eq. (1). In (b), the data were obtained by fitting the wTF-μ^+SR spectrum with Eq. (1) and the solid line represents the best fit using a Sigmoid function, which provides $T_{\rm C} = 151.11(4)$ K.

Figure 2(a) shows the temperature variation of the wTF-μ^+SR spectrum in $H_{\rm TF} = 30$ Oe at the vicinity of $T_{\rm C}$. The TF oscillation is heavily suppressed with decreasing temperature due to the appearance of large $\boldsymbol{H}_{\rm int}$. The wTF-μ^+SR spectrum was fitted by a combination of an exponentially relaxing cosine signal and two exponentially relaxing non-oscillatory signals, i.e., the signal from the paramagnetic phase and the longitudinal and transverse components of $\boldsymbol{H}_{\rm int}$ in the FM phase:

$$A_0 P_{\rm TF}(t) \quad = \quad A_{\rm TF} \cos(2\pi f_{\rm TF} t + \phi_{\rm TF}) \exp(-\lambda_{\rm TF} t)$$

$$+ \quad A_{\rm fast}\exp(-\lambda_{\rm fast}t) + A_{\rm tail}\exp(-\lambda_{\rm tail}t) \tag{1}$$

where A_0 denotes the initial asymmetry at $t = 0$, $P_{\rm TF}(t)$ denotes the μ^+ spin depolarization function in TF, $A_{\rm TF}$, $A_{\rm fast}$, and $A_{\rm tail}$ denote the asymmetries of the three signals, $f_{\rm TF}$ denotes the μ^+ spin precession frequency caused by TF, $\phi_{\rm TF}$ denotes the initial phase of the precession, and $\lambda_{\rm TF}$, $\lambda_{\rm fast}$, and $\lambda_{\rm tail}$ denote the exponential relaxation rate for the three signals. From the temperature dependence of $A_{\rm TF}$ [Fig. 2(b)], it is very clear that almost the whole volume of the $Y_2Co_{12}P_7$ sample enters an FM phase below $T_{\rm C} = 151$ K. This value agrees with $T_{\rm C}$ determined by magnetization measurements.

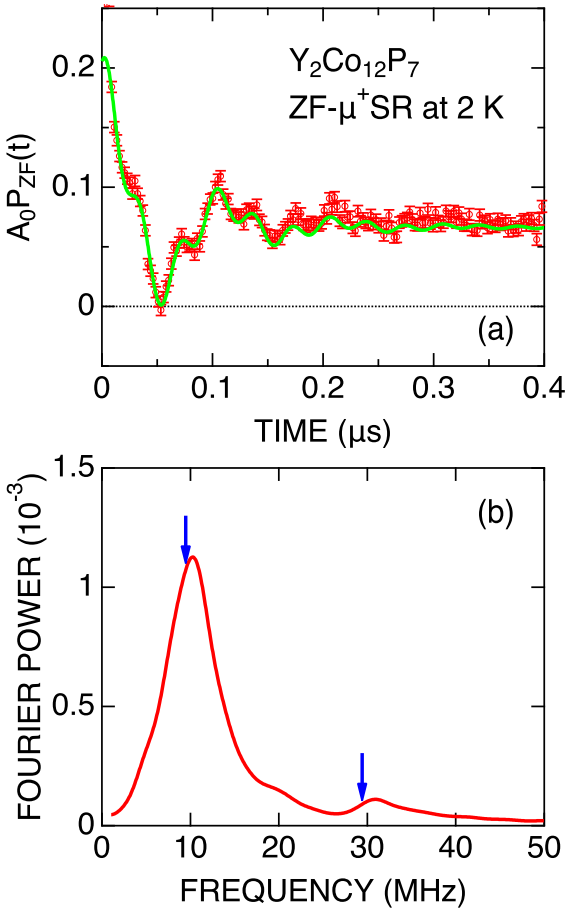

Figure 3. (a) The ZF-μ^+SR time spectrum for $Y_2Co_{12}P_7$ recorded at 2 K and (b) the Fourier transform frequency spectrum of (a). In (a), a solid line represents the best fit using Eq. (2).

Figure 3(a) shows the ZF-μ^+SR spectrum for $Y_2Co_{12}P_7$ recorded at the lowest temperature measured, i.e., 2 K. The observed complex oscillatory signal indicates the formation of static magnetic order in the FM phase with the presence of multiple muon sites. In fact, as seen in Fig. 3(b), the Fourier transform frequency spectrum of the ZF-μ^+SR time spectrum suggests the presence of two different muon sites in the lattice. Therefore, the ZF-μ^+SR spectrum was fitted with two exponentially relaxing cosine oscillations and an exponentially relaxing non-oscillatory

signal for the longitudinal component:

$$\begin{aligned} A_0 P_{\rm ZF}(t) &= \sum_{i=1}^{2} A_{{\rm FM}i} \cos(2\pi f_{{\rm FM}i} t + \phi_{\rm FM}) \exp(-\lambda_{{\rm FM}i} t) \\ &+ A_{\rm tail} \exp(-\lambda_{\rm tail} t), \end{aligned} \quad (2)$$

where $P_{\rm ZF}(t)$ denotes the μ^+ spin depolarization function in ZF, $A_{{\rm FM}i}$ and $A_{\rm tail}$ denote the asymmetries of the three signals, $f_{{\rm FM}i}$ denotes the μ^+ spin precession frequencies at the two muon sites caused by $\boldsymbol{H}_{\rm int}$, $\phi_{\rm FM}$ denotes the initial phase, and $\lambda_{{\rm FM}i}$ and $\lambda_{\rm tail}$ denote the exponential relaxation rate for the three signals. Note that the initial phase in cosine signal is common for the two signals. Among the temperature dependencies of the μ^+SR parameters in Fig. 4, both $f_{\rm FM1}$ and $f_{\rm FM2}$ exhibit a typical order parameter-like behavior and disappear at $T_{\rm C}$ [Fig. 4(a)], as expected.

The DFT calculations predicted the following three muon sites in the lattice [see Fig. 1]: $\mu_1 = (0.22950, 0.1639, 0)$, $\mu_2 = (0.41667, 0.3166, 0.5)$, and $\mu_3 = (0.08333, 0.2166, 0.5)$. The μ_1 site is the most preferable site, then, μ_2 follows μ_1 and μ_3 follows μ_2. While there are four Co sites in the lattice, the ordered moment of each site ($\boldsymbol{m}_{\mathbf{Co}i}$) is assumed as $\boldsymbol{m}_{\mathbf{Co1}} = (0, 0, 0.3)$ $\mu_{\rm B}$, $\boldsymbol{m}_{\mathbf{Co2}} = (0, 0, 0.3)$ $\mu_{\rm B}$, $\boldsymbol{m}_{\mathbf{Co3}} = (0, 0, 0.3)$ $\mu_{\rm B}$, and $\boldsymbol{m}_{\mathbf{Co4}} = (0, 0, 0.9)$ $\mu_{\rm B}$, based on the neutron work on $Pr_2Co_{12}P_7$, $Nd_2Co_{12}P_7$, and $Ho_2Co_{12}P_7$ [10]. Using these values, $\boldsymbol{H}_{\mathbf{dip}}$ for each site was estimated by dipole field calculates with dipelec [16]. The local spin density at each muon site [$\rho_{\rm spin}(\boldsymbol{r}_{\boldsymbol{\mu}})$] were also predicted with the DFT calculations: $\rho_{{\rm spin},\mu 1} = 0.01071$ $\mu_{\rm B}/{\rm \AA}^3$, $\rho_{{\rm spin},\mu 2} = -0.0004268$ $\mu_{\rm B}/{\rm \AA}^3$, and $\rho_{{\rm spin},\mu 3} = -0.0009780$ $\mu_{\rm B}/{\rm \AA}^3$. Thus, $\boldsymbol{H}_{\mathbf{hf}}$ of each muons site is obtained by $\boldsymbol{H}_{\mathbf{hf}} = \frac{8\pi}{3}\rho_{\rm spin}(\boldsymbol{r}_{\boldsymbol{\mu}})\frac{\boldsymbol{H}_{\mathbf{dip}}}{|\boldsymbol{H}_{\mathbf{dip}}|}$. The magnetization measurement provided the saturated magnetic moment (M_s) at 1.4 K to 3.7 $\mu_{\rm B}$/f.u. along the c-axis [11, 12], leading to $\boldsymbol{H}_{\mathbf{L}} = \frac{4\pi}{3}\boldsymbol{M}_{\boldsymbol{s}} = (0, 0, 561)$ Oe.

As seen in Fig. 5, the most suitable combination of $\boldsymbol{m}_{\mathbf{Co1}}$ and $\boldsymbol{m}_{\mathbf{Co4}}$ to explain the experimental results is $\boldsymbol{m}_{\mathbf{Co1}} = (0, 0, 0.20)$ $\mu_{\rm B}$ and $\boldsymbol{m}_{\mathbf{Co4}} = (0, 0, 0.61)$ $\mu_{\rm B}$, when $m_{\rm Co1z}/m_{\rm Co4z} = 1/3$ and $\boldsymbol{m}_{\mathbf{Co1}} = \boldsymbol{m}_{\mathbf{Co2}} = \boldsymbol{m}_{\mathbf{Co3}}$. The sum of $\boldsymbol{m}_{\mathbf{Co}i}$, i.e., $0.20 \times 9 + 0.61 \times 3 = 3.6$ $\mu_{\rm B}$/f.u., being consistent with the previous magnetization measurements result, i.e., $M_s = 3.7$ $\mu_{\rm B}$/f.u. at 1.4 K [11, 12]. Note that the $\boldsymbol{m}_{\mathbf{Co}i}$ values obtained with μ^+SR are about 68% of those estimated with neutron [10], indicating a unique power of μ^+SR to determine the ordered magnetic moments in ferromagnets. Note that the total estimation accuracy is restricted by the accuracy of the ordered magnetic moments determined with neutron [10]. In order to improve the accuracy, it would be preferable to measure a single crystal sample. Following upon the above results, we are attempting to study other $R_2Co_{12}P_7$ compounds with μ^+SR, although there are too many adjustable parameters for the prediction, such as, the magnitude and canting angle of each $\boldsymbol{m}_{\mathbf{Co}}$ and $\boldsymbol{m}_{\boldsymbol{R}}$.

4. Conclusion

By combining μ^+SR with DFT calculations, the ordered magnetic moments of Co in ferromagnetic $Y_2Co_{12}P_7$ were successfully determined. Then, we will move on the further challenge to conjecture the ordered magnetic moments of rare earth elements in $R_2Co_{12}P_7$.

5. Acknowledgments

We thank the staff of TRIUMF for help with the μ^+SR experiments (Proposal M1964). M.M., Y.S., and O.K.F. were partly supported by the Swedish Research Council (VR) through a neutron project grant (BIFROST, Dnr. 2016-06955). Y.S. also receive additional funding via a VR starting grant (Dnr. 2017-05078). E.N. is fully financed by the Swedish Foundation for Strategic Research (SSF) within the Swedish national graduate school in neutron scattering

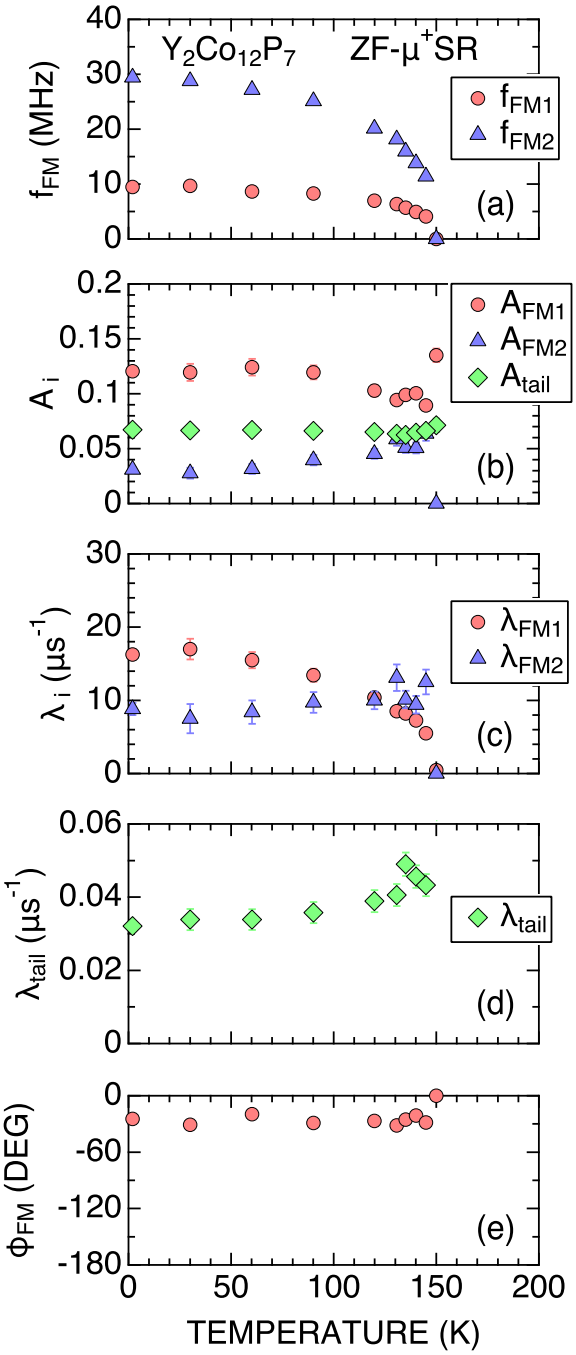

Figure 4. The temperature dependence of the μ^+SR parameters for $Y_2Co_{12}P_7$: (a) the two muon precession frequencies (f_{FM1} and f_{FM2}), (b) the three asymmetries (A_{FM1}, A_{FM2}, and A_{tail}), (c) the two relaxation rates (λ_{FM1} and λ_{FM2}), (d) the relaxation rate of the tail component (λ_{tail}), and (e) the initial phase (ϕ_{FM}). The data were obtained by fitting the ZF-μ^+SR spectrum with Eq. (2).

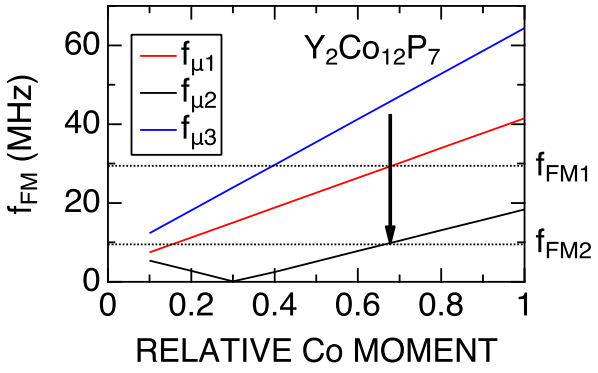

Figure 5. The predicted muon spin precession frequencies for the three muon sites as a function of the ordered Co moment. When the Relative Co moment is 1, the ordered Co moments are $\boldsymbol{m}_{\mathbf{Co1}} = \boldsymbol{m}_{\mathbf{Co2}} = \boldsymbol{m}_{\mathbf{Co3}} = (0, 0, 0.3)\ \mu_B$, and $\boldsymbol{m}_{\mathbf{Co4}} = (0, 0, 0.9)\ \mu_B$. When the Relative Co moment is 0.1, $\boldsymbol{m}_{\mathbf{Co1}} = \boldsymbol{m}_{\mathbf{Co2}} = \boldsymbol{m}_{\mathbf{Co3}} = (0, 0, 0.03)\ \mu_B$, and $\boldsymbol{m}_{\mathbf{Co4}} = (0, 0, 0.09)\ \mu_B$. Horizontal dotted lines represent the experimental results at 2 K. A vertical arrow represents a reasonable value of the Co moments (μ_1 and μ_2) to explain the experimental results.

(SwedNess). This work was supported by the Japan Society for the Promotion Science (JSPS) KAKENHI Grant No. JP17K06788, No. JP18H01863, and No. JP20K21149.

References

[1] Barth S, Albert E, Heiduk G, Möslang A, Weidinger A, Recknagel E and Buschow K H J 1986 *Phys. Rev. B* **33**(1) 430–436
[2] Yaouanc A and de Réotier P D 2011 Muon Spin Rotation, Relaxation, *and* Resonance, Application *to* Condensed Matter (New York: Oxford University Press)
[3] Forslund O K, Andreica D, Sassa Y, Nozaki H, Umegaki I, Nocerino E, Jonsson V, Tjernberg O, Guguchia Z, Shermadini Z, Khasanov R, Isobe M, Takagi H, Ueda Y, Sugiyama J and Månsson M 2019 *Scientific Reports* **9**(1) 1141
[4] Sugiyama J, Miwa K, Nozaki H, Kaneko Y, Hitti B, Arseneau D, Morris G D, Ansaldo E J and Brewer J H 2019 *Phys. Rev. Materials* **3**(6) 064402
[5] Forslund O K, Ohta H, Kamazawa K, Stubbs S L, Ofer O, Månsson M, Michioka C, Yoshimura K, Hitti B, Arseneau D, Morris G D, Ansaldo E J, Brewer J H and Sugiyama J 2020 *Phys. Rev. B* **102**(18) 184412
[6] Forslund O K, Andreica D, Ohta H, Imai M, Michioka C, Yoshimura K, Månsson M and Sugiyama J 2021 *Physica Scripta*
[7] Sugiyama J, Higemoto W, Andreica D, Forslund O K, Nocerino E, Månsson M, Sassa Y, Gupta R, Khasanov R, Ohta H and Nakamura H 2021 *Phys. Rev. B* **103**(10) 104418
[8] Jeitschko W, Braun D, Ashcraft R and Marchand R 1978 *Journal of Solid State Chemistry* **25** 309–313
[9] Reehuis M and Jeitschko W 1989 *Journal of Physics and Chemistry of Solids* **50** 563–569
[10] Reehuis M, Ouladdiaf B, Jeitschko W, Vomhof T, Zimmer B and Ressouche E 1997 *Journal of Alloys and Compounds* **261** 1–11
[11] Ohta H, Watanabe Y, Miyake A, Tokunaga M and Katori H A 2016 *Journal of the Japan Society of Powder and Powder Metallurgy* **63** 652–656
[12] Kato Y, Ohta H and Katori H A 2018 *Journal of the Japan Society of Powder and Powder Metallurgy* **65** 274–278
[13] Blaha P, Schwarz K, Tran F, Laskowski R, Madsen G K H and Marks L D 2020 *The Journal of Chemical Physics* **152** 074101
[14] Kalvius G M, Noakes D R and Hartmann O 2001 Handbook *on the* Physics *and* Chemistry *of* Rare Earths vol 32 (Amsterdam, Holland: North-Holland) chap 206, pp 55–451

[15] Suter A and Wojek B 2012 *Phys. Procedia* **30** 69–73 ISSN 1875-3892 proceedings of the 12th International Conference on Muon Spin Rotation, Relaxation and Resonance (μSR2011)
[16] Kojima K M, Yamanobe J, Eisaki H, Uchida S, Fudamoto Y, Gat I M, Larkin M I, Savici A, Uemura Y J, Kyriakou P P and et al 2004 *Phys. Rev. B* **70**(9) 094402